Cell

FoxOs Are Critical Mediators of Hematopoietic Stem Cell Resistance to Physiologic Oxidative Stress

Zuzana Tothova,[1,2,3,4] Ramya Kollipara,[2,7] Brian J. Huntly,[8] Benjamin H. Lee,[1,2,3] Diego H. Castrillon,[2,7,12] Dana E. Cullen,[1,3] Elizabeth P. McDowell,[1,3] Suzan Lazo-Kallanian,[7] Ifor R. Williams,[9] Christopher Sears,[1,10] Scott A. Armstrong,[10] Emmanuelle Passegué,[11] Ronald A. DePinho,[2,5,6,7] and D. Gary Gilliland[1,2,3,4,*]

[1] Division of Hematology, Department of Medicine, Brigham and Women's Hospital
[2] Department of Genetics
Harvard Medical School, Boston, MA 02115, USA
[3] Howard Hughes Medical Institute, Boston, MA 02115, USA
[4] Harvard-MIT Division of Health Sciences and Technology
[5] Center for Applied Cancer Science, Dana-Farber Cancer Institute
[6] Robert A. and Renee E. Belfer Foundation Institute for Innovative Cancer Science, Dana-Farber Cancer Institute
[7] Department of Medical Oncology, Dana-Farber Cancer Institute
Harvard Medical School, Boston, MA 02115, USA
[8] Department of Haematology, University of Cambridge, Cambridge Institute for Medical Research, Cambridge, CB2 2XY, UK
[9] Department of Pathology, Emory University School of Medicine, Atlanta, GA 30322, USA
[10] Division of Hematology/Oncology, Children's Hospital and Department of Pediatric Oncology, Dana-Farber Cancer Institute, Harvard Medical School, Boston, MA 02115, USA
[11] Developmental and Stem Cell Biology Program, University of California, San Francisco, CA 94143, USA
[12] Present address: Department of Pathology and Simmons Comprehensive Cancer Center, University of Texas Southwestern Medical Center, Dallas, TX 75390, USA.
*Correspondence: ggilliland@rics.bwh.harvard.edu
DOI 10.1016/j.cell.2007.01.003

SUMMARY

To understand the role of FoxO family members in hematopoiesis, we conditionally deleted *FoxO1*, *FoxO3*, and *FoxO4* in the adult hematopoietic system. *FoxO*-deficient mice exhibited myeloid lineage expansion, lymphoid developmental abnormalities, and a marked decrease of the lineage-negative Sca-1$^+$, c-Kit$^+$ (LSK) compartment that contains the short- and long-term hematopoietic stem cell (HSC) populations. *FoxO*-deficient bone marrow had defective long-term repopulating activity that correlated with increased cell cycling and apoptosis of HSC. Notably, there was a marked context-dependent increase in reactive oxygen species (ROS) in *FoxO*-deficient HSC compared with wild-type HSC that correlated with changes in expression of genes that regulate ROS. Furthermore, in vivo treatment with the antioxidative agent N-acetyl-L-cysteine resulted in reversion of the *FoxO*-deficient HSC phenotype. Thus, FoxO proteins play essential roles in the response to physiologic oxidative stress and thereby mediate quiescence and enhanced survival in the HSC compartment, a function that is required for its long-term regenerative potential.

INTRODUCTION

The FoxO (Forkhead O) subfamily of transcription factors plays an important role in diverse physiologic processes, including induction of cell cycle arrest, stress resistance, and apoptosis (Greer and Brunet, 2005). Four members of the FoxO subfamily, FoxO1, FoxO3, FoxO4, and FoxO6, are important downstream targets of the evolutionarily conserved PI3K-AKT pathway that transduces survival signals in response to growth factor stimulation. Growth factors or insulin activate the serine/threonine kinase AKT and trigger a spectrum of physiologic cellular responses, including cell proliferation, survival, growth, and metabolism, through downstream effectors, including BCL2 family members, caspases, NFκB, cell cycle regulators, mTOR, and FoxO transcription factors (Accili and Arden, 2004). AKT directly phosphorylates FoxO1, FoxO3, and FoxO4 at three conserved residues (Biggs et al., 1999; Brunet et al., 1999), resulting in nuclear exclusion and subsequent degradation. In the absence of growth factors or insulin, or with stress stimuli, FoxOs reside in the nucleus and are active as transcription factors, resulting in proapoptotic signaling via induction of TRAIL, FasL, and Bim (Brunet et al., 1999; Dijkers et al., 2000); cell cycle

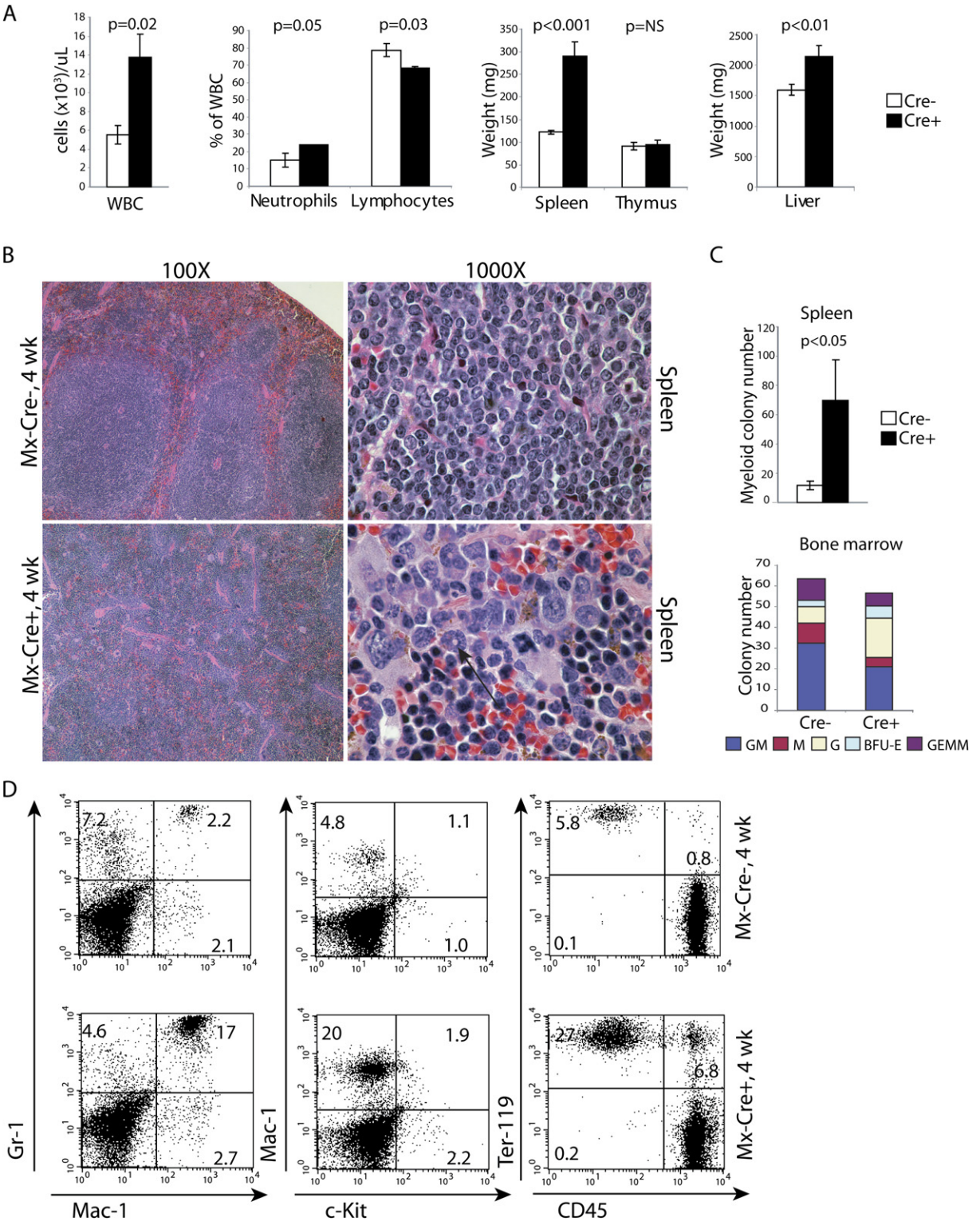

Figure 1. Loss of *FoxO* Leads to Myeloid Expansion in *MxCre⁺;FoxO1/3/4$^{L/L}$* Animals

(A) Bar graphs of total white blood cell count (WBC); percentage of neutrophils and lymphocytes; and splenic, thymic, and liver weights representative of *Mx-Cre⁺* or *Mx-Cre⁻;FoxO1/3/4$^{L/L}$* animals 4 weeks after pI-pC treatment. *FoxO*-deficient animals developed leukocytosis characterized by a relative neutrophilia and lymphopenia, and a significant increase in spleen and liver weights. Mean values ± SEM are plotted for a cohort of *Mx-Cre⁻* (n = 6) or *Mx-Cre⁺* (n = 7) animals.

arrest by activation of p27, p130, p21, and repression of Cyclin D expression (G1/S arrest) (Kops et al., 2002b; Medema et al., 2000; Seoane et al., 2004); activation of Cyclin G2 (G0/G1 arrest) (Martinez-Gac et al., 2004); and activation of Cyclin B and polo-like kinase (G2/M arrest) (Alvarez et al., 2001). In addition, the oxidative stress response is regulated in part by FoxO induction of MnSOD, catalase, and GADD45 (Kops et al., 2002a; Nemoto and Finkel, 2002; Tran et al., 2002), and has been linked to longevity and dauer formation in *C. elegans* (Honda and Honda, 1999; Lee et al., 2003; Murphy et al., 2003).

In the hematopoietic system, unrestrained PI3K signaling contributes to the pathogenesis of leukemia and autoimmune disease, whereas impaired PI3K signaling may result in immunodeficiency (Coffer and Burgering, 2004; Deane and Fruman, 2004). The importance of FoxOs in tumorigenesis in this context is underscored by findings that leukemia and lymphoma oncogenes, including BCR/ABL, FLT3-ITD, and NPM/ALK, mediate proliferation and survival signaling in part by activation of the PI3K-AKT pathway and inhibition of FoxOs (Gu et al., 2004; Komatsu et al., 2003; Scheijen et al., 2004). In addition, *FoxO3* and *FoxO4* are fusion partners of *MLL* in acute myeloid leukemias (AMLs) associated with t(6;11)(q21;q23) or t(X;11)(q13;q23), respectively (Borkhardt et al., 1997; Hillion et al., 1997; Parry et al., 1994). Furthermore, activation of the PI3K-AKT pathway through disruption of PTEN function results in AML in murine models (Yilmaz et al., 2006; Zhang et al., 2006).

Physiologic regulation of the dynamic balance between hematopoietic stem cell (HSC) self-renewal and differentiation is not fully understood, though recent studies underscore the importance of cell cycle, apoptosis, and oxidative stress response (reviewed in Attar and Scadden, 2004; Ito et al., 2004, 2006; Passegue et al., 2005). Although FoxOs influence each of these processes through their downstream effectors, deficiency of any one of the FoxO family members does not result in an overt hematopoietic phenotype. *FoxO1*-deficient animals show embryonic lethality at day E10.5 due to defects in angiogenesis (Furuyama et al., 2004; Hosaka et al., 2004); *FoxO3*-deficient animals become infertile due to global primordial follicle activation with subsequent oocyte exhaustion (Castrillon et al., 2003), as well as develop lymphoproliferation and inflammation in a *FoxO3* gene-trap model (Lin et al., 2004); and *FoxO4*-deficient animals are viable and have no overt phenotype (Hosaka et al., 2004). We hypothesized that FoxO family members are functionally redundant in the hematopoietic system, and therefore examined the effect of *FoxO* deficiency in hematopoietic stem and progenitor cells using mice engineered with conditional knockout alleles of *FoxO1*, *FoxO3*, and/or *FoxO4*, respectively.

RESULTS

Generation of *Mx-Cre^{+};FoxO1/3/4$^{L/L}$* Mice

Mice harboring the interferon-inducible transgene *Mx-Cre* in a *FoxO1/3/4$^{LoxP/LoxP}$* (hereafter *FoxO1/3/4$^{L/L}$*) background, or other genotypic combinations thereof (Figure S1), were generated. Cre expression and subsequent *FoxO* excision was induced in 4 week old mice, and subsequent analyses were performed 4–5 weeks after polyinosine-polycytidylic acid (pI-pC) treatment, at which time there was full excision of all three alleles in bone marrow (Figure S2A). pI-pC was also administered to *Mx-Cre^{-}* littermate controls.

Loss of FoxO Perturbs Myeloid and Lymphoid Lineages

Analysis of the peripheral blood 4 weeks after pI-pC induction showed an ~2-fold increase in the white blood cell (WBC) count in *Mx-Cre^{+};FoxO1/3/4$^{L/L}$* animals compared with *Mx-Cre^{-}* littermate controls that was attributable to an absolute and relative increase in the number of neutrophils (Figure 1A). There was also a significant increase in reticulocytes (5.8-fold increase, $p = 0.05$) without a significant difference in hemoglobin or hematocrit, and a slight decrease in platelet number (28% decrease; $p = 0.05$, data not shown). There was an ~2.5-fold increase in spleen weight ($p < 0.001$) and an ~1.5-fold increase in liver weight (Figure 1A, $p < 0.01$) in *FoxO*-deficient animals (see Table S1 in the Supplemental Data). Histopathologic analysis of *Mx-Cre^{+};FoxO1/3/4$^{L/L}$* showed mild to moderate expansion of the red pulp by extramedullary hematopoiesis comprised of maturing myeloid and erythroid cells (Figure 1B). Flow cytometry corroborated these findings, showing a 3.5-fold increase in the Gr1^{+}Mac1^{+} population ($p = 0.03$) and an ~6.1-fold increase in Ter119^{+}CD45^{-} population ($p = 0.04$) in the spleen (Figure 1D). Splenocytes derived from *Mx-Cre^{+};FoxO1/3/4$^{L/L}$* mice showed increased myeloid colony formation when plated in methylcellulose supplemented with hematopoietic cytokines compared with *Mx-Cre^{-};FoxO1/3/4$^{L/L}$* controls (Figure 1C). However, there was no serial replating activity, nor did colonies grow in the absence of growth factors.

(B) Splenic histology of representative *Mx-Cre^{-}* or *Mx-Cre^{+};FoxO1/3/4$^{L/L}$* mice 4 weeks after pI-pC treatment showed expansion of myeloid and erythroid elements in *Mx-Cre^{+}* animals. Arrow highlights maturing myeloid forms.

(C) Splenic cells from *Mx-Cre^{+}* excised animals (n = 3) at 4 weeks after pI-pC were more efficient at myeloid colony formation than *Mx-Cre^{-}* nonexcised littermates (n = 3). Unfractionated bone marrow plated on M3434 showed a consistent decrease in number, but no significant differences in the types, of colonies formed (GM, granulocyte macrophage; M, macrophage; G, granulocyte; BFU-E, burst-forming unit-erythroid; GEMM, granulocyte, erythroid, macrophage, megakaryocyte). Mean values ± SEM shown. A representative experiment is shown.

(D) Flow cytometric analysis of spleens from representative *Mx-Cre^{-}* or *Mx-Cre^{+};FoxO1/3/4$^{L/L}$* mice 4 weeks after pI-pC treatment confirmed an increased population of mature myeloid and erythroid cells in *Mx-Cre^{+}* animals [3.5-fold increase in Gr1^{+}Mac1^{+}, $p = 0.03$; 6.1-fold increase in Ter119^{+}CD45^{-}, $p = 0.04$; n = 7(*Mx-Cre^{+}*), n = 5 (*Mx-Cre^{-}*)].

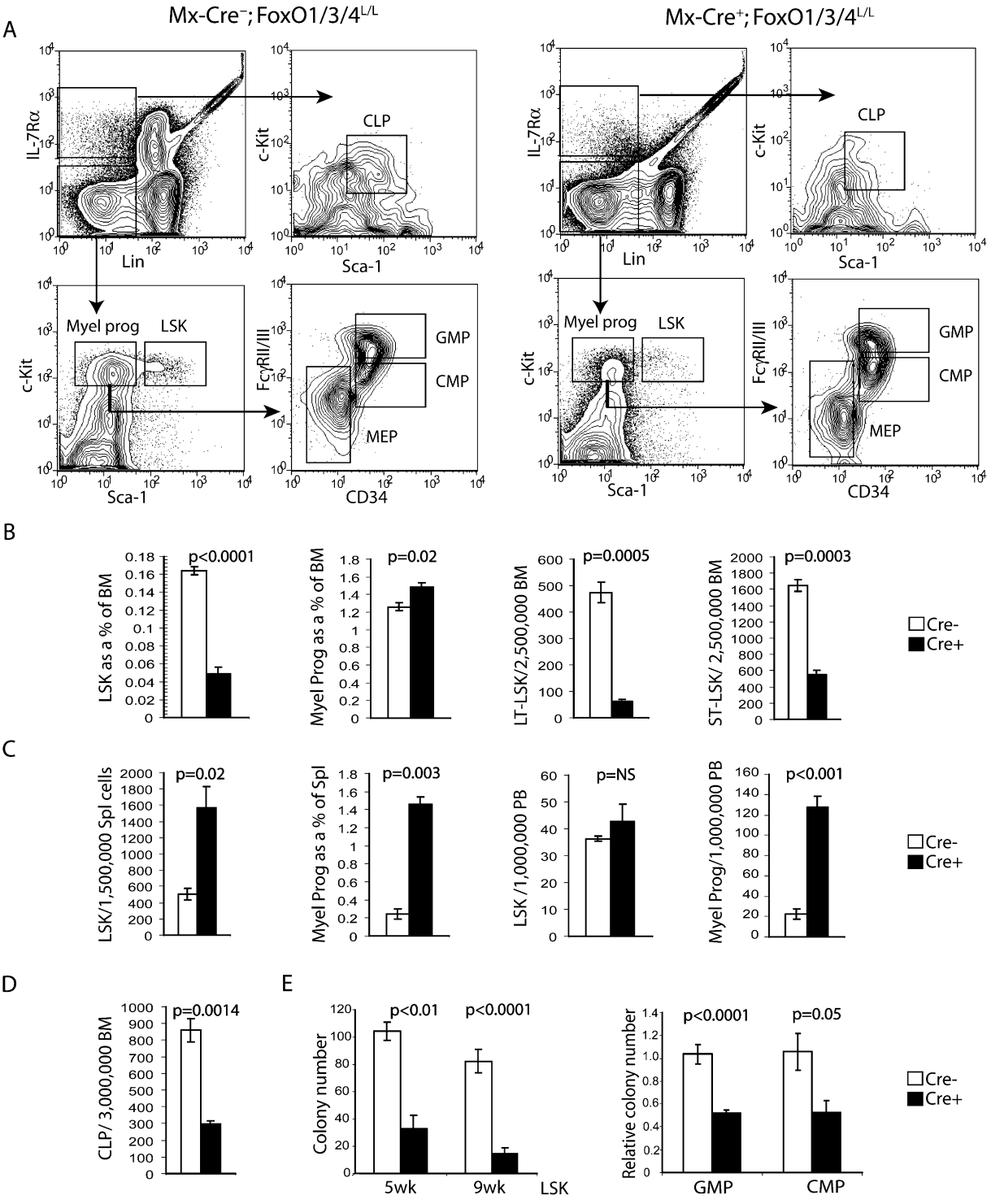

Figure 2. Reduced Size of HSC and CLP Compartments and Impaired Myeloid Colony-Forming Activity In Vitro in *FoxO*-Deficient Animals

(A) Multiparameter flow analysis showed a decrease in the size of the HSC(LSK) and CLP, but not myeloid progenitor, compartments in a representative *Mx-Cre*$^{+}$;*FoxO1/3/4*$^{L/L}$ mouse 4 weeks after pI-pC treatment.

(B) *FoxO*-deficient bone marrow exhibited a 4.6-fold decrease in the size of the HSC (Lin^{-} Sca-1^{+} c-Kit^{+}/LSK) compartment without a significant effect on the size of the myeloid progenitor (Lin^{-} c-Kit^{+} Sca-1^{-}) compartment. LT-LSK (Lin^{-} Sca-1^{+} c-Kit^{+} Flk2^{-}) population was more reduced in size than ST-LSK (Lin^{-} Sca-1^{+} c-Kit^{+} Flk2^{+}) population (8- versus 3-fold, respectively). n = 8 (*Mx-Cre*$^{+}$), n = 3 (*Mx-Cre*$^{-}$); mean values ± SEM are shown.

Although similar, findings in the bone marrow were more subtle than in the spleen (Figure S3). Long-term FoxO deficiency resulted in the development of a nonfatal myeloproliferative phenotype (see Supplemental Text and Figure S9 in the Supplemental Data).

There was aberrant differentiation in the B and T lymphoid compartments, including a relative and absolute decrease in peripheral blood lymphocytes in *Mx-Cre*$^{+}$*;FoxO1/3/4*$^{L/L}$ animals compared with *Mx-Cre*$^{-}$ littermate controls (Figure 1A). Flow cytometry showed a significant decrease in mature B cells in the bone marrow (~12 fold; $p = 0.02$) and spleen (~5 fold; $p < 0.0001$), respectively, of *Mx-Cre*$^{+}$*;FoxO1/3/4*$^{L/L}$ animals, with reduced numbers of pre-B and pro-B cells (Figure S4). There was a corresponding decrease in pre-B colony-forming activity in vitro in bone marrow cells derived from *Mx-Cre*$^{+}$*;FoxO1/3/4*$^{L/L}$ animals (2.7-fold decrease, $p < 0.001$, data not shown). In the T cell compartment, there was mild expansion of single positive $CD4^{+}CD3^{+}$ cells, reduction of double positive $CD4^{+}CD8^{+}$ cells, an increase in DN1 positive cells, and a decrease in DN3 positive cells, suggesting a modest block in T cell maturation at the DN1 → DN2 stage transition (Figure S5). Thus, loss of FoxO resulted in abnormalities in both myeloid and lymphoid compartments.

Quantitative and Qualitative Defects in the Hematopoietic Stem and Progenitor Compartments in *FoxO*-Deficient Mice

Abnormalities in both the myeloid and lymphoid compartments in *Mx-Cre*$^{+}$*;FoxO1/3/4*$^{L/L}$ animals prompted an examination of hematopoietic progenitor populations using multiparameter flow cytometry (Figure 2A). Wild-type stem cells and myeloid progenitors expressed *FoxO1*, *FoxO3*, and *FoxO4* as assessed by RT-PCR and qRT-PCR (Figure S2B). Although there was normal bone marrow cellularity in *Mx-Cre*$^{+}$*;FoxO1/3/4*$^{L/L}$ animals 4 weeks after pI-pC treatment, we observed a marked decrease in the HSC-enriched LSK compartment, defined as $Lin^{-}Sca\text{-}1^{+}c\text{-}Kit^{+}$ (4.6-fold, $p < 0.0001$), with minimal change in the size of the common myeloid progenitor (CMP), granulocyte-monocyte progenitor (GMP), or megakaryocyte-erythrocyte progenitor (MEP) subpopulations (Figure 2B). The LSK population (hereafter referred to as HSC) includes both long-term and short-term HSC (LT-HSC and ST-HSC, respectively), as well as multipotent progenitors (MPP). FoxO loss resulted in a preferential decrease in the size of the LT-HSC compartment ($Flk2^{-}$ LSK, 8-fold decrease; versus 3-fold decrease in number of $Flk2^{+}$ LSK, containing ST-HSC and MPP; Figure 2B) and in the common lymphoid progenitor (CLP) population (3-fold, $p = 0.001$, Figures 2A and 2D), whereas there was an increase in the number of myeloid progenitors in both spleen and peripheral blood (Figure 2C). Prospectively purified HSC, GMP, and CMP showed a statistically significant quantitative decrease in colony-forming activity in methylcellulose medium supplemented with hematopoietic cytokines (Figure 2E). Full excision was demonstrated for all three *FoxO* alleles in all colonies derived from sorted *Mx-Cre*$^{+}$*;FoxO1/3/4*$^{L/L}$ LSK cells (Figure S2C). Thus, loss of FoxO had profound effects on the size of the HSC and CLP compartments and caused qualitative defects in colony-forming activity in both stem cell and progenitor compartments.

FoxO-Null Bone Marrow Is Deficient in Long-Term Repopulating Ability In Vivo

Although there was complete excision of all *FoxO* alleles 4 weeks after pI-pC induction, there was reemergence of cells with unexcised *FoxO* alleles after 9 weeks in all lineages (data not shown). This finding suggested a competitive advantage for the rare hematopoietic progenitors in which excision did not occur. To test this hypothesis, noncompetitive and competitive repopulation assays were performed. We compared the repopulating ability of a congenic CD45.2 test population (*Mx-Cre*$^{+}$ or *Mx-Cre*$^{-}$*;FoxO1/3/4*$^{L/L}$) and a wild-type FVB CD45.1 support population transplanted into lethally irradiated F1 FVB/C57BL/6 CD45.1/CD45.2 recipients. Noncompetitive repopulation assays, in which 100% of *FoxO*-deficient or *FoxO*-wild-type bone marrow was transplanted into lethally irradiated recipients, showed a subtle increase in short-term repopulating activity of *Mx-Cre*$^{+}$*;FoxO1/3/4*$^{L/L}$ cells 4 weeks after transplantation. However, analysis of both the peripheral blood and bone marrow of recipients 16 weeks after transplant showed a statistically significant decrease in the long-term repopulating ability of these cells (Figure 3A, ~5-fold decrease, $p = 0.003$). These findings correlated with a dramatic reduction in the amount of HSC derived from *Mx-Cre*$^{+}$*;FoxO1/3/4*$^{L/L}$ bone marrow (Figure 3A, ~27-fold decrease, $p < 0.001$). The repopulation defect in *FoxO*-deficient cells was further accentuated by subsequent emergence of cells with wild-type *FoxO* alleles derived from the recipient. Enhanced short-term, but deficient long-term, repopulating ability of *Mx-Cre*$^{+}$*;FoxO1/3/4*$^{L/L}$ cells was also evident in competitive repopulation assays, in which test *FoxO*-deficient or *FoxO*-wild-type bone marrow was mixed with congenically distinct control wild-type bone marrow cells (Figure 3B). Taken together, these findings indicate that *FoxO1/3/4* deficiency results in perturbations in normal hematopoietic homeostasis. In addition, the response to

(C) Myeloid progenitors were expanded in both spleen and peripheral blood, and LSK population was modestly expanded in spleen. n = 5 (*Mx-Cre*$^{+}$), n = 3 (*Mx-Cre*$^{-}$); mean values ± SEM are shown.

(D) Number of CLP was 3-fold reduced in *FoxO*-deficient mice. n = 5 (*Mx-Cre*$^{+}$), n = 4 (*Mx-Cre*$^{-}$); mean values ± SEM shown.

(E) Plating of 200 sorted LSK or 1000 sorted progenitor (CMP and GMP) cells from *Mx-Cre*$^{-}$ or *Mx-Cre*$^{+}$*;FoxO1/3/4*$^{L/L}$ mice 5 or 9 weeks after pI-pC on M3434 medium showed a marked decrease in myeloid colony-forming ability of *FoxO*-deficient cells on Day 10. n = 3 (LSK; *Mx-Cre*$^{-}$ or *Mx-Cre*$^{+}$); n = 6 (GMP; *Mx-Cre*$^{+}$); n = 3 (GMP; *Mx-Cre*$^{-}$); n = 3 (CMP; *Mx-Cre*$^{-}$ or *Mx-Cre*$^{+}$); mean values ± SEM shown.

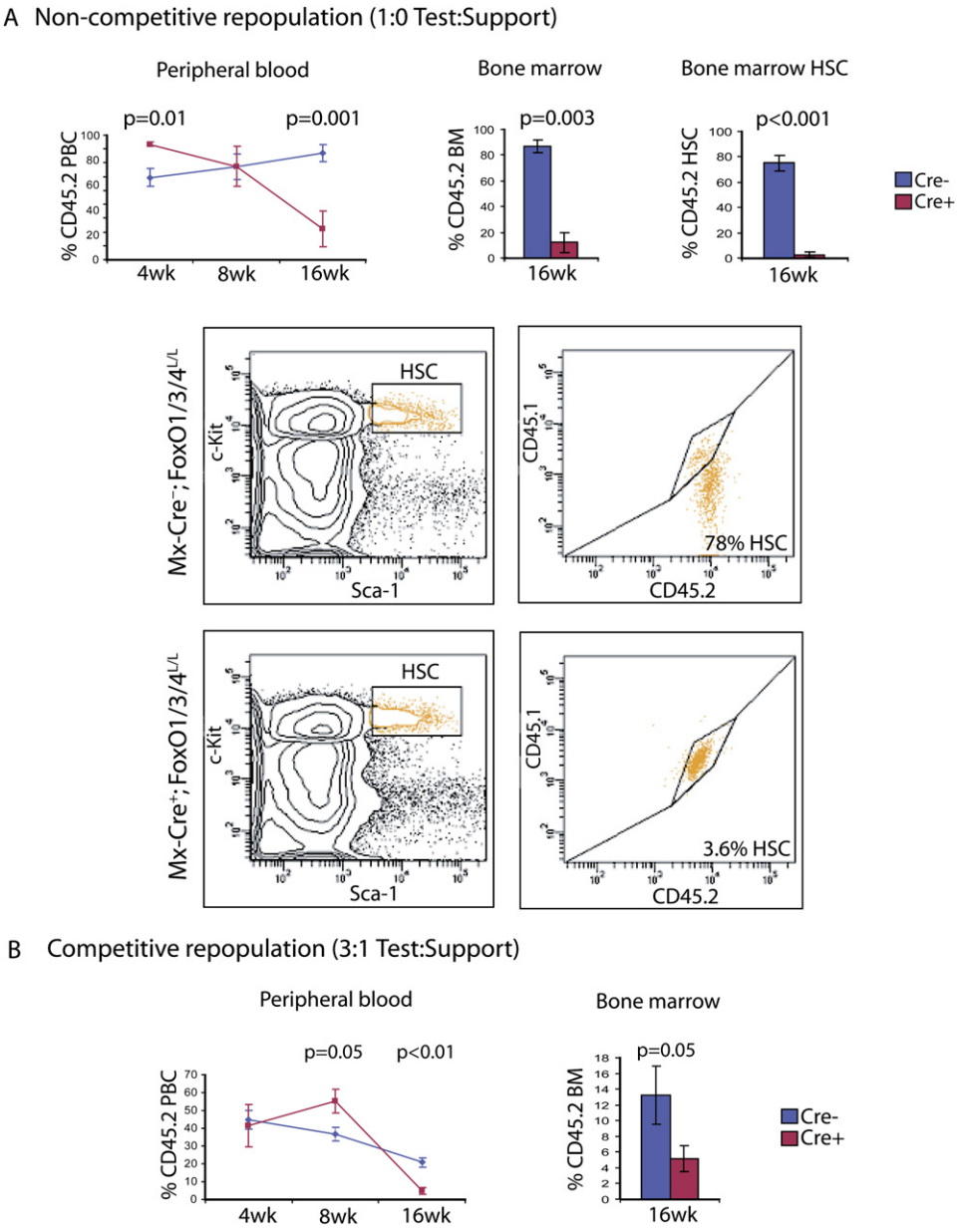

Figure 3. *FoxO*-Deficient Bone Marrow Shows Enhanced Short-Term and Deficient Long-Term Repopulating Ability In Vivo

Recipient mice (CD45.1+/CD45.2+) were analyzed for contribution of the *Mx-Cre*$^{+}$ or *Mx-Cre*$^{-}$*;FoxO1/3/4*$^{L/L}$ (test, CD45.2+) population-derived and wild-type (support, CD45.1+) population-derived cells in peripheral blood and bone marrow at 4, 8, and 16 weeks after transplantation in (A) noncompetitive or (B) competitive repopulation assays. *FoxO*-deficient bone marrow showed increased short-term (weeks 4, 8) and decreased long-term (week 16) repopulating ability, with decreased numbers of *FoxO*-deficient bone marrow-derived HSC cells 16 weeks post-transplant. n = 4 (nonc.; 4 or 8 wk); n = 8 (nonc., 16 wk); n = 4 (comp.; 4 or 8 or 16 wk); mean values ± SEM shown.

certain stressors, even noncompetitive transplantation into secondary congenic recipient mice, is severely impaired in the HSC compartment.

FoxO-Deficient HSC, but Not Myeloid Progenitor Cells, Show Abnormal Cell Cycle Regulation

To further characterize the quantitative and qualitative defects in the HSC compartment of *Mx-Cre*$^{+}$*;FoxO1/3/4*$^{L/L}$ mice, cell cycle analysis was performed. There was a striking HSC-restricted phenotype, with a marked increase in the number of *Mx-Cre*$^{+}$*;FoxO1/3/4*$^{L/L}$ HSC in S/G2/M (~2-fold; $p < 0.001$) compared with *Mx-Cre*$^{-}$ control HSC populations (Figures 4A and 4B). This was accompanied by a significant reduction in the G0/G1 fraction of *Mx-Cre*$^{+}$*;FoxO1/3/4*$^{L/L}$ HSC (~2-fold; $p < 0.001$). There was also a significant increase in the number of HSCs in G1

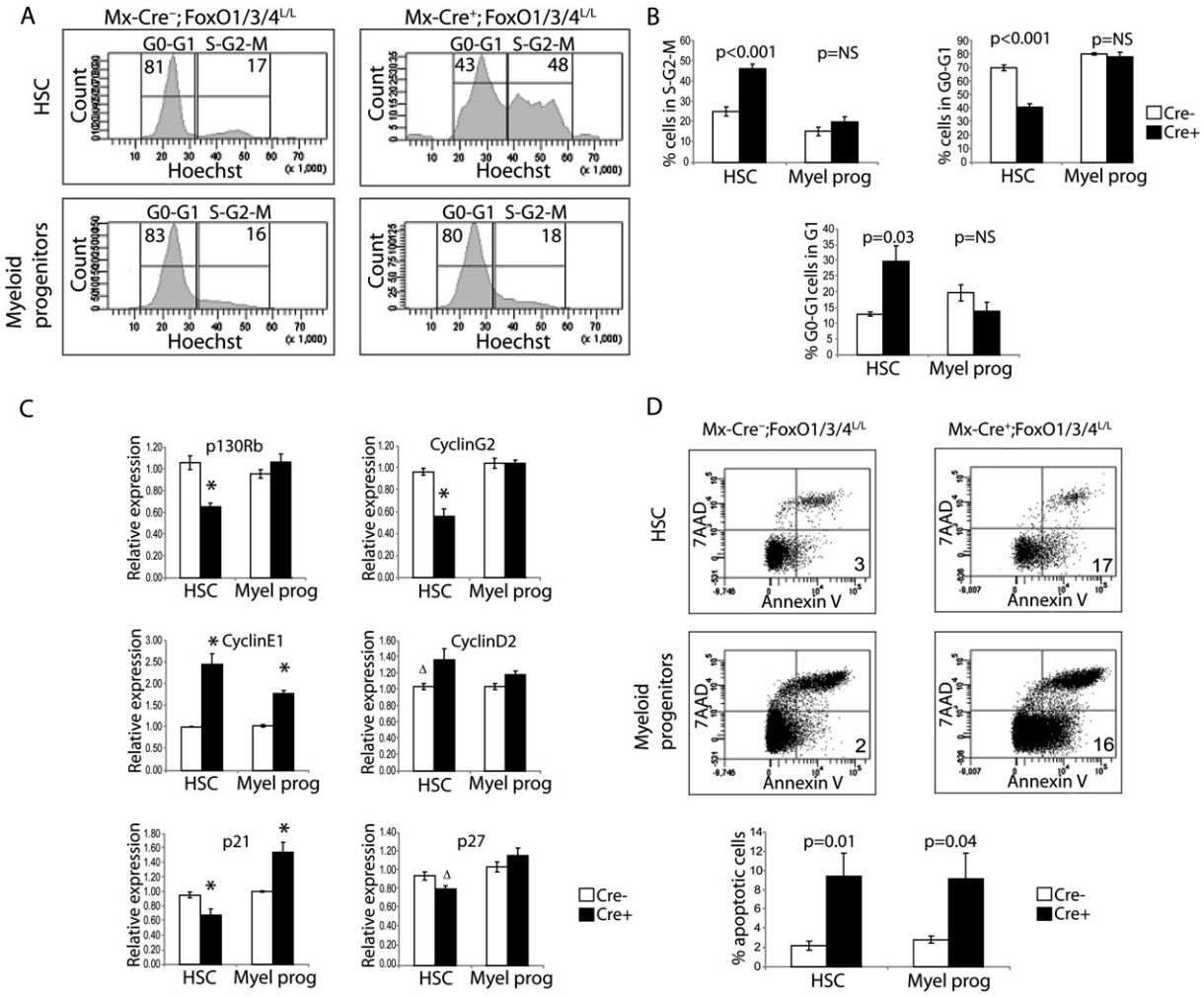

Figure 4. FoxO Deficiency Results in an Increased HSC-Specific Entry into the S/G2/M and G1 Phases of the Cell Cycle and Increased Apoptosis in HSC and Myeloid Progenitor Compartments In Vivo

(A and B) Bone marrow isolated from *Mx-Cre*$^{+}$ (n = 7) or *Mx-Cre*$^{-}$ (n = 3) *FoxO1/3/4*$^{L/L}$ animals 5 weeks after pI-pC was stained for stem and progenitor markers, and cell cycle status was determined using Hoechst 33342 and Pyronin Y staining. (A) Representative flow cytometry data showing that *FoxO*-deficient HSC(LSK), but not myeloid progenitors, exhibit an increased entry into S/G2/M, with a proportional decrease in the G0/G1 phase. (B) *FoxO*-deficient HSC(LSK), but not myeloid progenitors, have a 2-fold increased entry into S/G2/M, a concomitant 2-fold decrease in the fraction of G0/G1 cells, and a 2-fold increased entry into the G1 phase.

(C) Bone marrow cells from two sets of pooled *Mx-Cre*$^{+}$ or *Mx-Cre*$^{-}$*;FoxO1/3/4*$^{L/L}$ animals 4 weeks after pI-pC were sorted as HSC(LSK) and myeloid progenitors, and RNA was isolated and used to synthesize cDNA. The results represent the mean ± SEM of triplicate measurements performed on three sorted sets of HSC populations. Levels of expression were standardized to β-actin and expression level in the *Mx-Cre*$^{-}$ HSC or progenitors was set to 1 for each gene examined. p130/Rb, Cyclin G2, p21, and Cyclin E1 had markedly altered expression levels in the HSC compartment. (*) denotes $p < 0.05$, $^{\Delta}$ denotes p = 0.08 and 0.06 for CyclinD2 HSC and p27 HSC, respectively.

(D) Bone marrow isolated from *Mx-Cre*$^{+}$ (n = 6) or *Mx-Cre*$^{-}$ (n = 6) *FoxO1/3/4*$^{L/L}$ animals 5 weeks post pI-pC was stained for stem and progenitor markers, and apoptosis was assessed using 7-AAD and Annexin-V staining. Representative flow cytometry data showed that *FoxO*-deficient HSC and myeloid progenitors had increased levels of apoptosis relative to wild-type littermates. *FoxO*-deficient HSC and progenitors exhibited an ~4-fold increased entry into apoptosis. n = 6 (*Mx-Cre*$^{+}$ or *Mx-Cre*$^{-}$); mean values ± SEM are shown.

phase (~2-fold; p = 0.03), suggesting their increased exit from quiescence (Figure 4B). In contrast, myeloid progenitor populations showed no cell cycle differences between *Mx-Cre*$^{+}$ and *Mx-Cre*$^{-}$*;FoxO1/3/4*$^{L/L}$ animals (Figures 4A and 4B). These findings were maintained over 13 weeks after induction with pI-pC, and were reproduced when *FoxO*-deficient bone marrow was transplanted into wild-type recipients (data not shown), indicating a cell-autonomous effect of *FoxO* deficiency on cell cycle regulation in HSC.

Stem Cell-Specific Entry into S/G2/M Is Correlated with Altered Expression of FoxO Target Genes

Expression analysis of cell cycle intermediates regulated by FoxOs correlated with observed HSC-specific cell

cycle abnormalities. For example, in the *Mx-Cre*$^{+}$*;FoxO1/3/4*$^{L/L}$ animals, there was an HSC-specific downregulation of Cyclin G2, p130/Rb, p27, and p21; and upregulation of Cyclin D2 (Figure 4C). Thus, the abnormalities in cell cycle observed in vivo correlate with changes in expression of FoxO cell cycle regulatory targets.

Increased Apoptosis in *FoxO*-Deficient HSC and Myeloid Progenitors

Mx-Cre^{+}*;FoxO1/3/4*$^{L/L}$ HSC and myeloid progenitor cells exhibited increased rates of apoptosis (Figure 4D; ~4-fold for both HSC and progenitors, $p = 0.01$ and $p = 0.04$, respectively). Increased apoptosis was maintained for at least 13 weeks after excision and was reproduced when *FoxO*-deficient bone marrow was transplanted into wild-type recipients, indicating that these are, at least in part, cell-autonomous effects of FoxOs that regulate genes governing cellular survival. However, unlike cell cycle abnormalities, increased apoptosis was not restricted to the HSC compartment, but was also present in mature, lineage-positive myeloid populations (data not shown).

Loss of All Three *FoxO* Alleles Is Required for Full Potentiation of the Cell Cycle and Apoptosis Phenotypes

To determine which member(s) of the FoxO subfamily mediated cell cycle and apoptosis defects observed in the stem cell compartment of triply-deficient *FoxO* animals, we analyzed animals deficient in single or all combinations of two of the three members of the FoxO subfamily 5 weeks after pI-pC, respectively (*Mx-Cre*$^{+}$*;FoxO1*$^{L/L}$, *Mx-Cre*$^{+}$*;FoxO3*$^{L/L}$, *Mx-Cre*$^{+}$*;FoxO4*$^{L/L}$, *Mx-Cre*$^{+}$*;FoxO1/3*$^{L/L}$, *Mx-Cre*$^{+}$*;FoxO1/4*$^{L/L}$, or *Mx-Cre*$^{+}$*;FoxO3/4*$^{L/L}$). There were no phenotypic differences between pI-pC-treated *Mx-Cre*$^{+}$ and *Mx-Cre*$^{-}$ littermates of single-knockout mice (Figure 5A). Similarly, double-knockout mice showed no HSC abnormalities, with the exception of *Mx-Cre*$^{+}$*;FoxO1/3*$^{L/L}$ mice, which showed increased levels of apoptosis (Figure 5B). These data indicate that loss of all three *FoxO* alleles is necessary to fully manifest the cell cycle and apoptosis phenotypes. This functional redundancy demonstrates a critical role for FoxOs in the hematopoietic system, and explains why overt hematopoietic phenotypes were not observed in single-knockout animals.

An HSC-Restricted Increase in Reactive Oxygen Species in *FoxO*-Deficient Mice

We next assessed whether the *FoxO*-deficient HSC phenotype was associated with increased levels of reactive oxygen species (ROS) (Kops et al., 2002a). HSC was purified by multiparameter flow cytometry from *Mx-Cre*$^{+}$ or *Mx-Cre*$^{-}$*;FoxO1/3/4*$^{L/L}$ animals 6 weeks after pI-pC induction, and the intracellular concentration of ROS was measured by 2′-7′-dichlorofluorescein diacetate (DCF-DA) staining. We noted a marked increase in ROS levels in HSC derived from *Mx-Cre*$^{+}$*;FoxO1/3/4*$^{L/L}$ animals compared with that derived from *Mx-Cre*$^{-}$ animals (~2.5 fold, $p < 0.0001$, Figures 6A and 6B).

To gain insight into the basis for increased levels of ROS in the HSC compartment, we performed global gene expression microarray analysis on prospectively purified HSC derived from *Mx-Cre*$^{+}$ or *Mx-Cre*$^{-}$*;FoxO1/3/4*$^{L/L}$ animals, respectively. We first generated a list of genes involved in ROS metabolism, including those responsive to oxidative stress, ROS, hydrogen peroxide, oxygen radicals, and to superoxide, respectively (ROS gene list, see Supplemental Materials and Methods and Table S2). We then analyzed the gene expression data using gene set enrichment analysis (GSEA; Krivtsov et al., 2006; Subramanian et al., 2005), a computational method that determines if a defined gene set shows differential expression between two biological states (http://www.broad.mit.edu/gsea/). When comparing HSC derived from *Mx-Cre*$^{+}$ or *Mx-Cre*$^{-}$*;FoxO1/3/4*$^{L/L}$ animals (Figure S6A), we observed enrichment in expression of ROS genes in wild-type HSC compared with *FoxO*-deficient HSC. A subset of the ROS gene list, defined as the "leading edge" set of genes, accounted for the enrichment (Figure S6A; Subramanian et al., 2005). Leading edge genes more highly expressed in wild-type HSC than *FoxO*-deficient HSC included superoxide dismutase genes *Sod1* and *Sod3* (Figure S6A). These findings indicate that *FoxO* deficiency in the HSC compartment results in aberrant expression of genes that regulate ROS.

To determine whether the increase of ROS in *FoxO*-deficient HSC was restricted to the stem cell compartment, we measured ROS levels in myeloid progenitors. In contrast to the HSC compartment, there was no difference in ROS levels between *FoxO*-deficient and wild-type myeloid progenitors (Figures 6A and 6B). Thus, the aberrant increase of ROS in *FoxO*-deficient mice was restricted to the stem cell compartment.

However, levels of ROS in myeloid progenitor cells were much higher than those in HSC, in both wild-type and *FoxO*-deficient animals (Figure 6A). One explanation for the marked increase in ROS in myeloid progenitors relates to the function of their terminally differentiated progeny, neutrophils and monocytes. These cells are professional generators of ROS, which is a part of their physiologic role in initial host defense mechanisms against infection. Thus, the increase in ROS in myeloid progenitors might be the consequence of a developmental program that enables ROS production associated with commitment to differentiation in the myeloid lineage. This could be enacted mechanistically either by downregulation of FoxO with the transition from HSC to myeloid progenitors, or by engagement of a developmental transcriptional program that is FoxO-independent.

To delineate between these possible explanations, we first analyzed *FoxO* expression by qRT-PCR, and observed no statistically significant differences in the levels of expression of *FoxO1*, *FoxO3*, or *FoxO4* between wild-type HSC and myeloid progenitors (Figure S2B). Thus, the difference in ROS levels between HSC and myeloid progenitors was not explained as a consequence of decreased *FoxO* family member expression. We next

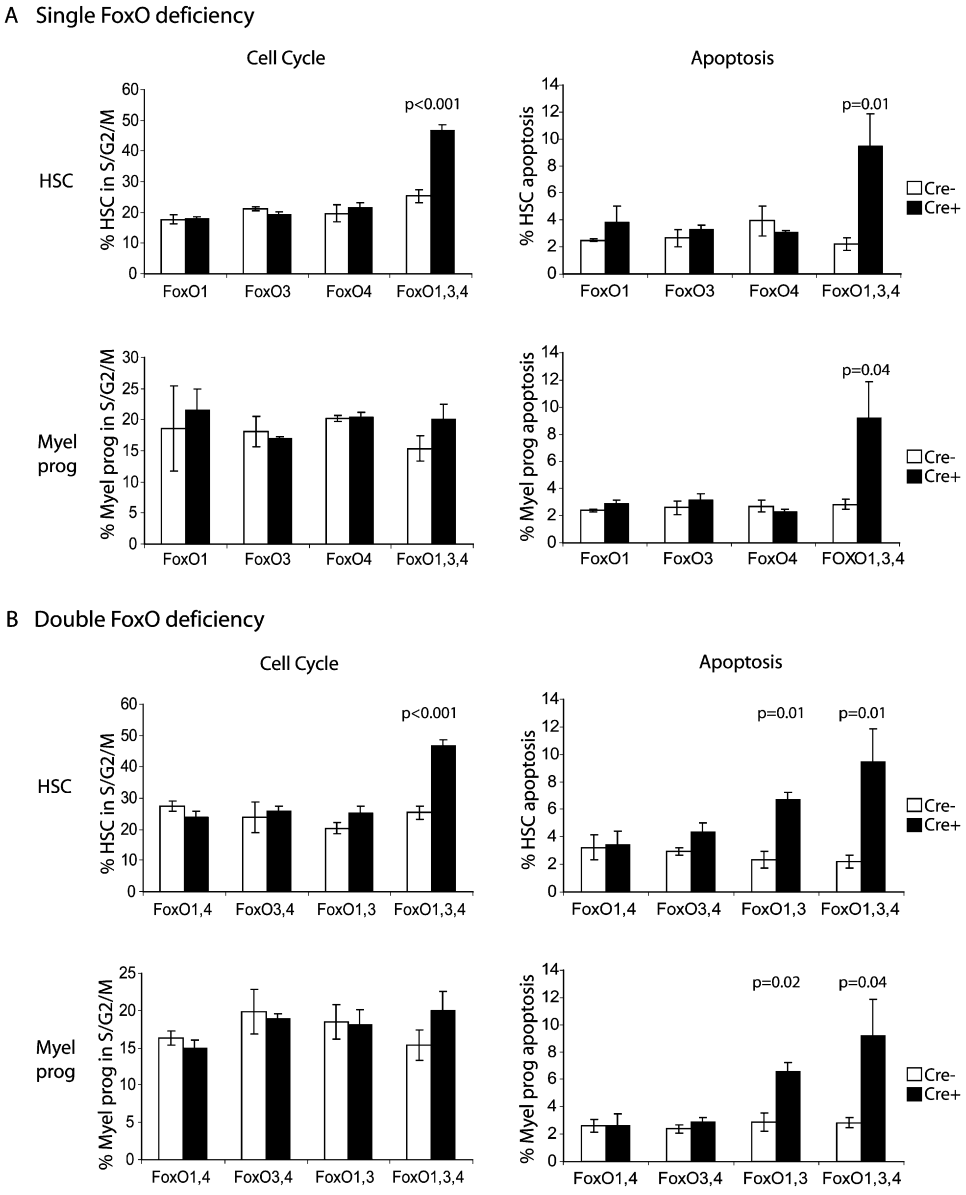

Figure 5. Loss of All Three *FoxO* Alleles Is Required for Full Potentiation of the Cell Cycle and Apoptosis Phenotypes in the HSC Compartment

Bone marrow cells isolated from *Mx-Cre*$^{+}$ or *Mx-Cre*$^{-}$ single- (A) or double- (B) floxed *FoxO* animals 5 weeks after pI-pC were stained for HSC or progenitor markers, and cell cycle and apoptosis were measured with Hoechst 33342 and Pyronin Y, and 7-AAD/Annexin-V staining, respectively. n = 3 in each group; mean values ± SEM shown.

analyzed the microarray data sets derived from wild-type or *FoxO*-deficient HSC and myeloid progenitors to explore the possibility that myeloid progenitors employ a *FoxO*-independent developmental transcriptional program to regulate ROS. We first compared expression of the ROS gene set described above in wild-type HSC with that of wild-type myeloid progenitors using GSEA. There was enrichment of a subset of ROS leading edge genes, consistent with engagement of a developmental program associated with the transition from HSC to myeloid progenitors (Figure S6B and Figure 6C). We next compared *FoxO*-deficient HSC with *FoxO*-deficient myeloid progenitors and observed similar ROS gene set enrichment (Figure S6C). When we compared the genes whose expression was enhanced during the transition from HSC to myeloid progenitors in wild-type cells to the genes with increased expression during the same transition in *FoxO*-deficient cells, there was a high degree of overlap (Figures 6D and 6F). This observation is consistent with a ROS developmental program that is activated with

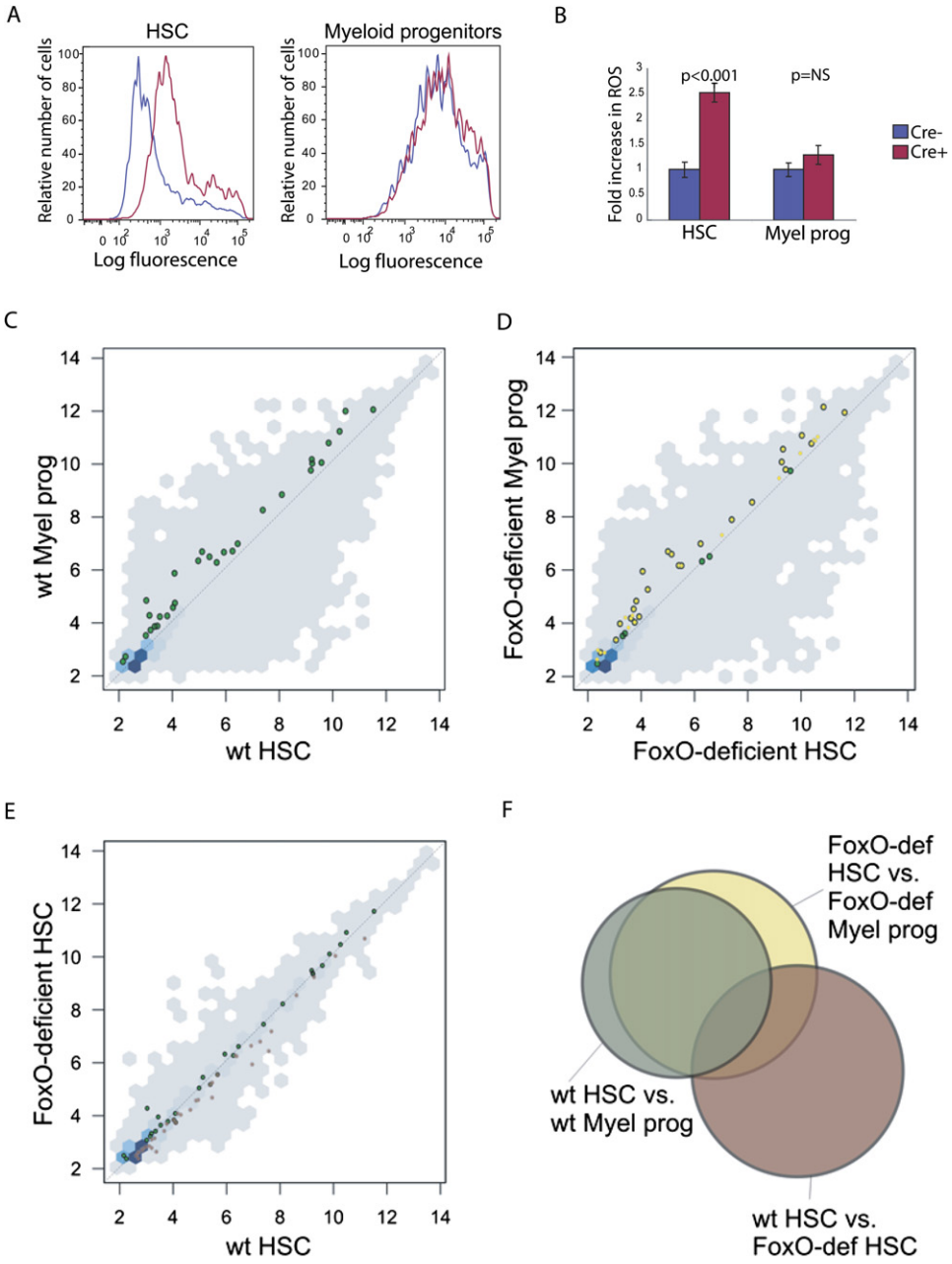

Figure 6. GSEA Analysis of the HSC-Restricted Increase of ROS in *FoxO*-Deficient Mice

(A and B) HSC or myeloid progenitors from *Mx-Cre*$^{+}$ or *Mx-Cre*$^{-}$*;FoxO1/3/4*$^{L/L}$ were stained with DCF-DA to measure intracellular ROS. *FoxO*-deficient HSC, but not myeloid progenitors, showed increased levels of ROS. Mean values ± SEM shown; n = 3 in each group.

(C) A comparison of log-transformed gene expression data is shown for wild-type myeloid progenitors (MP) versus wild-type LSK(HSC). GSEA assessed enrichment of genes involved in ROS metabolism (Figure S6B). There was enrichment of a subset of genes in the myeloid progenitors. The enriched genes (the leading edge in Figure S6B) are shown as green circles.

(D) GSEA performed using the ROS gene set on data from *FoxO*-deficient MP versus *FoxO*-deficient HSC. There was enrichment in a subset of genes in the *FoxO*-deficient MP that were similar to those in Figure 6C. The enriched genes (leading edge of the GSEA in Figure S6C) are shown as yellow circles. The yellow circles with a black outline are enriched in *FoxO*-deficient MP and wild-type MP. The green circles are enriched only in wild-type MP.

(E) GSEA performed using the ROS gene set on data from *FoxO*-deficient HSC versus wild-type HSC. There is enrichment of a subset of genes in the wild-type HSC. The enriched genes (leading edge of Figure S6A) are shown in red. The genes enriched in MP are shown in green.

(F) Venn diagram of the enriched genes in all three comparisons. Note that the genes whose expression is increased in wild-type and *FoxO*-deficient MP as compared with HSC are largely the same, whereas genes enriched in the wild-type HSC compared with *FoxO*-deficient HSC are unique.

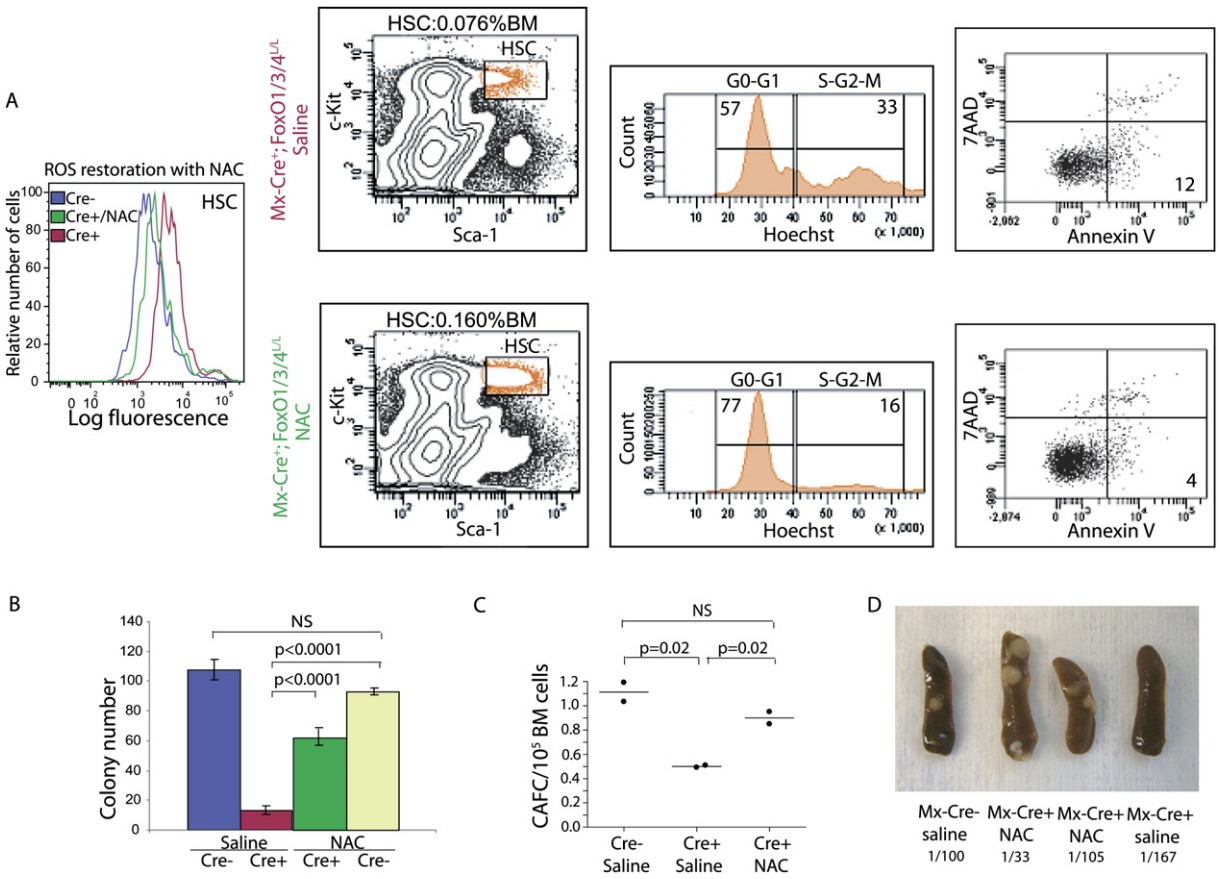

Figure 7. Antioxidant Treatment of *FoxO*-Deficient Mice In Vivo Reverses Increased ROS Levels as well as Quantitative and Qualitative Defects of *FoxO*-Deficient HSC

(A) In vivo NAC treatment resulted in rescue of the HSC phenotype, including restoration of the levels of ROS, HSC pool size, HSC cycling profile, and apoptosis in the HSC compartment.

(B) In vivo NAC treatment restored Day 10 myeloid colony-forming ability of HSC(LSK) sorted from *Mx-Cre*$^{+}$;*FoxO1/3/4*$^{L/L}$ animals. Two hundred HSC cells isolated from *Mx-Cre*$^{-}$ or *Mx-Cre*$^{+}$;*FoxO1/3/4*$^{L/L}$ mice after a 5 week long treatment with NAC in vivo were plated on M3434 in duplicate. n = 2 (*Mx-Cre*$^{-}$/saline or NAC); n = 3 (*Mx-Cre*$^{+}$/saline); n = 4 (*Mx-Cre*$^{+}$/NAC); mean values ± SEM shown.

(C) Long-term cobblestone area-forming cell (CAFC) assay showed rescue of CAFC production in bone marrow cells isolated from *Mx-Cre*$^{+}$;*FoxO1/3/4*$^{L/L}$ mice after a 5 week long treatment with NAC in vivo. n = 2 (*Mx-Cre*$^{-}$/saline); n = 2 (*Mx-Cre*$^{+}$/saline); n = 2 (*Mx-Cre*$^{+}$/NAC); actual and mean values shown.

(D) CFU-S colony-forming ability was restored in HSC cells isolated from *Mx-Cre*$^{+}$;*FoxO1/3/4*$^{L/L}$ mice after 2 week long NAC treatment in vivo. Spleens of animals in a representative experiment are shown. n = 2 (*Mx-Cre*$^{-}$/saline); n = 2 (*Mx-Cre*$^{+}$/saline); n = 4 (*Mx-Cre*$^{+}$/NAC); n = 2 (*Mx-Cre*$^{-}$/NAC). Duplicate recipient mice were transplanted with 500 HSC cells from each donor. Frequency of CFU-S is calculated as 1/(number of cells transplanted/number of colonies observed).

the transition from HSC to myeloid progenitors and is independent of FoxO. Examples of genes in this category include myeloperoxidase, eosinophil peroxidase, and glutathione peroxidase 3 (Figures S6B and S6C). In contrast, there was little overlap among ROS genes that demonstrated decreased expression in *FoxO*-deficient HSC and the genes activated as part of the developmental program in myeloid progenitors (Figures 6E and 6F). Taken together, these data indicate that there is an HSC-restricted requirement for FoxO for regulation of response to physiologic oxidative stress, and that FoxO-independent, ROS-associated transcriptional programs are engaged in the transition from HSC to myeloid progenitors.

Reduction of ROS Levels In Vivo Using Antioxidants Rescues the *FoxO*-Deficient HSC Phenotype

We next asked whether increased ROS was causally implicated in the severe phenotypic defects in the HSC compartment. We attempted rescue of the *FoxO*-deficient HSC phenotype in vivo using antioxidants. *Mx-Cre*$^{+}$ or *Mx-Cre*$^{-}$;*FoxO1/3/4*$^{L/L}$ animals were treated daily with the antioxidant N-acetyl-L-cysteine (NAC) or control saline solution for 5 weeks immediately after the last pI-pC administration, and then analyzed for qualitative and quantitative changes in the stem cell compartment. Reduction of ROS in the HSC compartment (Figure 7A) resulted in reversion of the HSC phenotype, including restoration of the HSC compartment size, reestablishment of normal

stem cell cycling, and normalization of HSC apoptosis (Figure 7A). Measurement of ROS levels as a quantitative pharmacodynamic metric of NAC efficacy showed variation in response, as anticipated from the use of a chemically reactive antioxidant administered in vivo by subcutaneous injection. However, variance in pharmacodynamic response enabled analysis of the dose-response relationship between the degree of restoration of ROS levels and the attenuation of the phenotypic defects in HSC. There was a highly statistically significant relationship between NAC-mediated restoration of ROS levels and restoration of the phenotype in HSC ($p = 0.0072$, Figure S7), providing further support that increased ROS is responsible for the *FoxO*-deficient HSC phenotype.

Several assays confirmed functional rescue of HSC from NAC-treated, *FoxO*-deficient animals. First, there was restoration of levels of expression of FoxO targets in prospectively purified HSC from *MxCre*$^{+}$*;FoxO1/3/4*$^{L/L}$ animals after in vivo treatment with NAC, including cell cycle intermediates (Figure S8A). Second, NAC treatment of *MxCre*$^{+}$*; FoxO1/3/4*$^{L/L}$ animals resulted in statistically significant rescue of myeloid colony-forming activity of purified HSC (Figure 7B). Third, NAC treatment rescued long-term HSC function in the cobblestone area-forming cell assay (CAFC; Figure 7C). Fourth, in vivo assays of colony-forming units in the spleen (CFU-S) that measure short-term repopulating activity in the HSC compartment of *FoxO*-deficient animals showed a statistically significant functional rescue with NAC treatment (Figure 7D), whereas NAC had no effect on CFU-S of wild-type HSC (data not shown).

Taken together, these data indicate that FoxOs play critical and functionally redundant roles in the maintenance of the HSC compartment, and that the HSC phenotype in *FoxO*-deficient animals can be attributed at least in part to impaired detoxification of ROS.

DISCUSSION

Loss of three members of the FoxO subfamily of transcription factors, *FoxO1*, *FoxO3*, and *FoxO4,* results in a severe defect in the HSC compartment. Although a semblance of hematopoietic homeostasis can be achieved by *FoxO*-deficient HSC, there is a striking decrease in HSC number, and even the relatively modest stress of transplantation into secondary recipient mice results in rapid extinction of *FoxO*-deficient HSC.

To investigate the mechanistic basis for the defect in *FoxO*-deficient HSC, we first assessed the effect of *FoxO* deficiency on the cell cycle. Flow cytometric data and qRT-PCR data indicate that *FoxO*-deficient HSC are driven out of quiescence into the cell cycle. Taken together with the reduced number of HSC and impaired long-term repopulating activity, these findings suggest that *FoxO* deficiency enforces cell fate decisions in which HSC are driven into cycle and terminal differentiation at the expense of self-renewal.

There was also an aberrant increase in ROS in the HSC compartment of *FoxO*-deficient animals. GSEA confirmed a decrease in expression of a subset of ROS genes in *FoxO*-deficient HSC compared with wild-type HSC. To determine whether aberrant ROS was causally implicated in the *FoxO*-deficient HSC phenotype, we assessed reversion of phenotype with in vivo administration of NAC. Remarkably, NAC rescued the *FoxO*-deficient HSC phenotype, restoring the size and function of the HSC compartment as well as correcting the abnormalities in cell cycle and apoptosis. Thus, most, if not all, phenotypic manifestations of *FoxO* deficiency are the consequence of increased ROS in the HSC compartment. Taken together, these genetic data show that FoxOs are essential and functionally redundant in the maintenance of quiescence and integrity of the HSC compartment. Furthermore, these data demonstrate a genetic link between FoxOs and protection from physiologic oxidative stress in the hematopoietic compartment, and the essentiality of ROS regulation for a spectrum of cellular functions that include cell cycle control and regulation of apoptosis.

In contrast with the HSC compartment, myeloid progenitors were normal in number and showed no cell cycle defects or differences in ROS levels in *FoxO*-deficient animals. Increased apoptosis in the absence of increased ROS suggests that apoptotic effects may be ROS-independent in this compartment. Thus, the *FoxO*-deficient phenotype is restricted to the HSC compartment, and therefore the effect of *FoxO* deficiency is highly context-dependent—even the most immediate progeny of the HSC compartment, the myeloid progenitors, no longer require FoxO for most physiological functions.

There was also a marked increase in ROS levels with the transition from HSC to myeloid progenitors that was not affected by *FoxO* deficiency, suggesting a FoxO-independent developmental program that regulates ROS levels in myeloid progenitors. GSEA supports the existence of a developmentally regulated program that is engaged with the transition from HSC to myeloid progenitors. In particular, *FoxO*-deficient or wild-type myeloid progenitors show enrichment for the same subset of ROS genes; this gene set is different from that observed in the HSC compartment. These data suggest that there is a subset of ROS genes that are regulated by FoxO in the HSC compartment and serve to decrease levels of ROS and their deleterious effects on HSC survival and function. With the transition to myeloid progenitors, a developmentally regulated transcriptional program is activated that enables differentiation of myeloid progenitors into professional ROS-generating cells. These findings thus provide new insights into developmental regulation of ROS during hematopoietic development and highlight the delicate balancing act in myeloid progenitors between activation of ROS for professional purposes and the deleterious effects of ROS on cell survival, and may explain in part why myeloid cells are the shortest-lived of all hematopoietic constituents.

We also observed decreased expression of *ATM* and increased expression of its target, *p16*, in *FoxO*-deficient HSC (Figure S8B). Furthermore, ATM levels were restored

with NAC treatment in vivo (Figure S8B). It has been reported that ATM may influence HSC integrity through regulation of p16 and ROS (Ito et al., 2004). Our data further suggest a link between FoxO and ATM, and that ATM and its target, p16, may lie downstream of FoxO. In addition, increased levels of ROS have been reported to mediate association of β-catenin and FoxO; β-catenin is purported to enhance FoxO's role in inhibiting cell cycle progression (Essers et al., 2005). It is thus possible that ROS-enhanced binding of FoxO to β-catenin is an effector of FoxO-induced quiescence in the HSC compartment, and serves to counteract the deleterious effects of ROS on HSC self-renewal.

These data also have interesting implications for recent reports of the HSC phenotype in *Pten*-deficient mice, which is nearly identical to the phenotype in *FoxO*-deficient mice (Yilmaz et al., 2006; Zhang et al., 2006). Rapamycin reverts the phenotype of *Pten*-deficient HSC, suggesting that mTOR signaling is responsible for the HSC phenotype (Yilmaz et al., 2006). However, genetic data in this report indicate that the HSC phenotype is most likely attributable to loss of function of FoxO, rather than activation of mTOR, in the setting of *Pten*-deficiency. The basis for the rapamycin effect in the *Pten*-deficient background is not clear, but it could be due to off-target effects of rapamycin that affect FoxO function, or differential effects of rapamycin on the mTORC1 versus mTORC2 complexes that influence AKT activity (Sarbassov et al., 2006).

Finally, it is of interest to relate these effects of *FoxO* deficiency in the hematopoietic system to other contexts. For example, isolated *FoxO3* deficiency results in oocyte exhaustion and infertility due to global activation of the primordial ovarian follicle (Castrillon et al., 2003). These phenotypic attributes are similar to those observed in the hematopoietic system, and suggest that FoxOs may play an important role in the maintenance and integrity of stem cell compartments in a broad spectrum of tissues. In addition, there are similarities between the role of FoxOs in regulation of quiescence and longevity of HSC in vertebrates and regulation of dauer diapause and life span determination in *C. elegans* by the FoxO ortholog DAF-16. Together, these findings provide strong support for the relevance of FoxO in longevity of HSC and perhaps in the broader spectrum of adult tissue stem cells in invertebrates and vertebrates.

FoxO transcription factors thus play a critical role in hematopoietic homeostasis by regulating the HSC compartment. We propose that under homeostatic conditions, FoxO transcription factors maintain self-renewal of HSC. Our data are consistent with the hypothesis that FoxOs cooperate to affect quiescence of HSC by regulation of the cell cycle, inhibition of apoptosis, and mediation of resistance to physiologic oxidative stress. These findings suggest that FoxOs are important in maintaining the long-term regenerative potential of the HSC compartment, and that analysis of the role of FoxOs in other adult and embryonic stem cell compartments may yield insights into the physiology and diseases of the renewing organ systems of long-lived species, including humans.

EXPERIMENTAL PROCEDURES

Generation of *Mx-Cre*$^{+}$*;FoxO1/3/4*$^{L/L}$ Mice

See the Supplemental Data.

Flow Cytometry

LSK, CMP, GMP, MEP, and CLP populations were analyzed and sorted with a FACSAria instrument (Becton Dickinson, Mountain View, CA) (Akashi et al., 2000; Kondo et al., 1997). Apoptosis was assayed by staining freshly harvested bone marrow cells with lineage, stem, and progenitor markers, followed by Annexin-V and 7-AAD staining. Cell cycle analysis was assessed as previously reported (Cheng et al., 2000). ROS levels were measured by sorting 5000 LSKs or 50,000 myeloid progenitors and staining with 5 μM DCF-DA (2′-7′-dichlorofluorescein diacetate, Molecular Probes) for 30 min at 37°C followed by flow cytometric analysis (Ito et al., 2004). Additional details are provided in the Supplemental Data.

Colony Assays

Myeloid and pre-B colony-plating assays were performed in methylcellulose-based medium M3434 and M3630 (Stem Cell Technologies, Vancouver, BC, Canada) with 2×10^4 bone marrow and spleen cells and 5×10^4 bone marrow cells, plated in duplicate and scored for colony formation at 10 and 14 days, respectively. Serial replating was performed 7 days after plating. For CFU-S assays, 500 LSK cells were isolated from *Mx-Cre*$^{+}$ and *Mx-Cre*$^{-}$*;FoxO1/3/4*$^{L/L}$ animals that were treated daily with NAC or saline for 2 or 4 weeks, and injected into lateral tail veins of lethally irradiated F1 FVB/C57BL/6 recipient mice in duplicate, which were subsequently treated with NAC (600 mg/kg; i.p.) or saline once a day. Day 12 CFU-S assay was carried out as described (Morrison and Weissman, 1994).

Transplantation Assays

Bone marrow cells from *Mx-Cre*$^{-}$ or *Mx-Cre*$^{+}$*;FoxO1/3/4*$^{L/L}$ mice (both CD45.2 at the CD45 locus) alone (noncompetitive transplants) or mixed with bone marrow cells from wild-type FVB mice (CD45.1) (competitive transplants) were injected into lateral tail veins of lethally irradiated F1 FVB/C57BL/6 recipient animals (CD45.1/CD45.2; 2X600rad). Peripheral blood collected at 4, 8, and 16 weeks, and bone marrow from mice at 16 weeks was analyzed for contribution of CD45 congenic and lineage markers by flow cytometry. Noncompetitive and competitive transplants were carried out with three and two sets of donor mice in independent experiments, respectively, with four to eight recipient mice per group in each experiment.

N-acetyl-L-cysteine Administration In Vivo

Five-week-old *Mx-Cre*$^{+}$ and *Mx-Cre*$^{-}$*;FoxO1/3/4*$^{L/L}$ animals were treated daily with NAC (100 mg/kg; Sigma) or saline solution by subcutaneous administration, starting 1 day after last pI-pC induction, and were subsequently analyzed after 5 weeks of treatment.

Gene Expression Analysis

qRT-PCR was performed as previously described (Passegue et al., 2005) and primers are available upon request (FoxO1, FoxO3, FoxO4). All reactions were performed in an ABI-7000 sequence detection system using SYBR Green PCR Core reagents according to the manufacturer's instructions (Applied Biosystems). Details of the microarray and GSEA analysis are provided in the Supplemental Data.

CAFC Assay

Assays were performed as described (Moore et al., 1997). Briefly, bone marrow cells isolated from *Mx-Cre*$^{+}$ and *Mx-Cre*$^{-}$*;FoxO1/3/4*$^{L/L}$ animals after 5 weeks of in vivo treatment with saline or NAC were plated

on AFT024 stromal monolayers in limiting dilutions in 96-well plates and maintained for 4 weeks with weekly medium hemi-depletion. Cultures containing bone marrow cells isolated from NAC-treated animals were supplemented with NAC (100 μM) daily. CAFC frequency was determined using L-Calc software (StemCell Technologies). Statistical significance of differences between parameters measured for *Mx-Cre*$^{+}$ or *Mx-Cre*$^{-}$*;FoxO1/3/4*$^{L/L}$ animals was assessed using a two-tailed unpaired t test.

Supplemental Data

The Supplemental Data for this article can be found online at http://www.cell.com/cgi/content/full/128/2/325/DC1/.

ACKNOWLEDGMENTS

We thank David Scadden and Lynda Chin for critical review of the manuscript; Jennifer Adelsperger, Rachel Okabe, Sandy Moore, Allison Coburn, and Maricel Gozo for technical assistance; Joe Growney and other members of the Gilliland and DePinho labs for valuable discussion; and John Daley for assistance with flow cytometry. B.J.P.H. is a senior clinical fellow of the Medical Research Council (UK). D.H.C. is a Sidney Kimmel Foundation Scholar and supported by the Mary Kay Ash Foundation. This work was supported in part by NIH grants (D.G.G., R.A.D.) and the Leukemia and Lymphoma Society (D.G.G.). D.G.G. is an Investigator of the Howard Hughes Medical Institute.

Received: June 3, 2006
Revised: October 17, 2006
Accepted: January 7, 2007
Published: January 25, 2007

REFERENCES

Accili, D., and Arden, K.C. (2004). FoxOs at the crossroads of cellular metabolism, differentiation, and transformation. Cell *117*, 421–426.

Akashi, K., Traver, D., Miyamoto, T., and Weissman, I.L. (2000). A clonogenic common myeloid progenitor that gives rise to all myeloid lineages. Nature *404*, 193–197.

Alvarez, B., Martinez, A.C., Burgering, B.M., and Carrera, A.C. (2001). Forkhead transcription factors contribute to execution of the mitotic programme in mammals. Nature *413*, 744–747.

Attar, E.C., and Scadden, D.T. (2004). Regulation of hematopoietic stem cell growth. Leukemia *18*, 1760–1768.

Biggs, W.H., 3rd, Meisenhelder, J., Hunter, T., Cavenee, W.K., and Arden, K.C. (1999). Protein kinase B/Akt-mediated phosphorylation promotes nuclear exclusion of the winged helix transcription factor FKHR1. Proc. Natl. Acad. Sci. USA *96*, 7421–7426.

Borkhardt, A., Repp, R., Haas, O.A., Leis, T., Harbott, J., Kreuder, J., Hammermann, J., Henn, T., and Lampert, F. (1997). Cloning and characterization of AFX, the gene that fuses to MLL in acute leukemias with a t(X;11)(q13;q23). Oncogene *14*, 195–202.

Brunet, A., Bonni, A., Zigmond, M.J., Lin, M.Z., Juo, P., Hu, L.S., Anderson, M.J., Arden, K.C., Blenis, J., and Greenberg, M.E. (1999). Akt promotes cell survival by phosphorylating and inhibiting a Forkhead transcription factor. Cell *96*, 857–868.

Castrillon, D.H., Miao, L., Kollipara, R., Horner, J.W., and DePinho, R.A. (2003). Suppression of ovarian follicle activation in mice by the transcription factor Foxo3a. Science *301*, 215–218.

Cheng, T., Rodrigues, N., Shen, H., Yang, Y., Dombkowski, D., Sykes, M., and Scadden, D.T. (2000). Hematopoietic stem cell quiescence maintained by p21cip1/waf1. Science *287*, 1804–1808.

Coffer, P.J., and Burgering, B.M. (2004). Forkhead-box transcription factors and their role in the immune system. Nat. Rev. Immunol. *4*, 889–899.

Deane, J.A., and Fruman, D.A. (2004). Phosphoinositide 3-kinase: diverse roles in immune cell activation. Annu. Rev. Immunol. *22*, 563–598.

Dijkers, P.F., Medema, R.H., Lammers, J.W., Koenderman, L., and Coffer, P.J. (2000). Expression of the pro-apoptotic Bcl-2 family member Bim is regulated by the forkhead transcription factor FKHR-L1. Curr. Biol. *10*, 1201–1204.

Essers, M.A., de Vries-Smits, L.M., Barker, N., Polderman, P.E., Burgering, B.M., and Korswagen, H.C. (2005). Functional interaction between beta-catenin and FOXO in oxidative stress signaling. Science *308*, 1181–1184.

Furuyama, T., Kitayama, K., Shimoda, Y., Ogawa, M., Sone, K., Yoshida-Araki, K., Hisatsune, H., Nishikawa, S., Nakayama, K., Ikeda, K., et al. (2004). Abnormal angiogenesis in Foxo1 (Fkhr)-deficient mice. J. Biol. Chem. *279*, 34741–34749.

Greer, E.L., and Brunet, A. (2005). FOXO transcription factors at the interface between longevity and tumor suppression. Oncogene *24*, 7410–7425.

Gu, T.L., Tothova, Z., Scheijen, B., Griffin, J.D., Gilliland, D.G., and Sternberg, D.W. (2004). NPM-ALK fusion kinase of anaplastic large-cell lymphoma regulates survival and proliferative signaling through modulation of FOXO3a. Blood *103*, 4622–4629.

Hillion, J., Le Coniat, M., Jonveaux, P., Berger, R., and Bernard, O.A. (1997). AF6q21, a novel partner of the MLL gene in t(6;11)(q21;q23), defines a forkhead transcriptional factor subfamily. Blood *90*, 3714–3719.

Honda, Y., and Honda, S. (1999). The daf-2 gene network for longevity regulates oxidative stress resistance and Mn-superoxide dismutase gene expression in Caenorhabditis elegans. FASEB J. *13*, 1385–1393.

Hosaka, T., Biggs, W.H., 3rd, Tieu, D., Boyer, A.D., Varki, N.M., Cavenee, W.K., and Arden, K.C. (2004). Disruption of forkhead transcription factor (FOXO) family members in mice reveals their functional diversification. Proc. Natl. Acad. Sci. USA *101*, 2975–2980.

Ito, K., Hirao, A., Arai, F., Matsuoka, S., Takubo, K., Hamaguchi, I., Nomiyama, K., Hosokawa, K., Sakurada, K., Nakagata, N., et al. (2004). Regulation of oxidative stress by ATM is required for self-renewal of haematopoietic stem cells. Nature *431*, 997–1002.

Ito, K., Hirao, A., Arai, F., Takubo, K., Matsuoka, S., Miyamoto, K., Ohmura, M., Naka, K., Hosokawa, K., Ikeda, Y., and Suda, T. (2006). Reactive oxygen species act through p38 MAPK to limit the lifespan of hematopoietic stem cells. Nat. Med. *12*, 446–451.

Komatsu, N., Watanabe, T., Uchida, M., Mori, M., Kirito, K., Kikuchi, S., Liu, Q., Tauchi, T., Miyazawa, K., Endo, H., et al. (2003). A member of Forkhead transcription factor FKHRL1 is a downstream effector of STI571-induced cell cycle arrest in BCR-ABL-expressing cells. J. Biol. Chem. *278*, 6411–6419.

Kondo, M., Weissman, I.L., and Akashi, K. (1997). Identification of clonogenic common lymphoid progenitors in mouse bone marrow. Cell *91*, 661–672.

Kops, G.J., Dansen, T.B., Polderman, P.E., Saarloos, I., Wirtz, K.W., Coffer, P.J., Huang, T.T., Bos, J.L., Medema, R.H., and Burgering, B.M. (2002a). Forkhead transcription factor FOXO3a protects quiescent cells from oxidative stress. Nature *419*, 316–321.

Kops, G.J., Medema, R.H., Glassford, J., Essers, M.A., Dijkers, P.F., Coffer, P.J., Lam, E.W., and Burgering, B.M. (2002b). Control of cell cycle exit and entry by protein kinase B-regulated forkhead transcription factors. Mol. Cell. Biol. *22*, 2025–2036.

Krivtsov, A.V., Twomey, D., Feng, Z., Stubbs, M.C., Wang, Y., Faber, J., Levine, J.E., Wang, J., Hahn, W.C., Gilliland, D.G., et al. (2006). Transformation from committed progenitor to leukaemia stem cell initiated by MLL-AF9. Nature *442*, 818–822.

Lee, S.S., Kennedy, S., Tolonen, A.C., and Ruvkun, G. (2003). DAF-16 target genes that control C. elegans life-span and metabolism. Science *300*, 644–647.

Lin, L., Hron, J.D., and Peng, S.L. (2004). Regulation of NF-kappaB, Th activation, and autoinflammation by the forkhead transcription factor Foxo3a. Immunity *21*, 203–213.

Martinez-Gac, L., Marques, M., Garcia, Z., Campanero, M.R., and Carrera, A.C. (2004). Control of cyclin G2 mRNA expression by forkhead transcription factors: novel mechanism for cell cycle control by phosphoinositide 3-kinase and forkhead. Mol. Cell. Biol. *24*, 2181–2189.

Medema, R.H., Kops, G.J., Bos, J.L., and Burgering, B.M. (2000). AFX-like Forkhead transcription factors mediate cell-cycle regulation by Ras and PKB through p27kip1. Nature *404*, 782–787.

Moore, K.A., Ema, H., and Lemischka, I.R. (1997). In vitro maintenance of highly purified, transplantable hematopoietic stem cells. Blood *89*, 4337–4347.

Morrison, S.J., and Weissman, I.L. (1994). The long-term repopulating subset of hematopoietic stem cells is deterministic and isolatable by phenotype. Immunity *1*, 661–673.

Murphy, C.T., McCarroll, S.A., Bargmann, C.I., Fraser, A., Kamath, R.S., Ahringer, J., Li, H., and Kenyon, C. (2003). Genes that act downstream of DAF-16 to influence the lifespan of Caenorhabditis elegans. Nature *424*, 277–283.

Nemoto, S., and Finkel, T. (2002). Redox regulation of forkhead proteins through a p66shc-dependent signaling pathway. Science *295*, 2450–2452.

Parry, P., Wei, Y., and Evans, G. (1994). Cloning and characterization of the t(X;11) breakpoint from a leukemic cell line identify a new member of the forkhead gene family. Genes Chromosomes Cancer *11*, 79–84.

Passegue, E., Wagers, A.J., Giuriato, S., Anderson, W.C., and Weissman, I.L. (2005). Global analysis of proliferation and cell cycle gene expression in the regulation of hematopoietic stem and progenitor cell fates. J. Exp. Med. *202*, 1599–1611.

Sarbassov, D.D., Ali, S.M., Sengupta, S., Sheen, J.H., Hsu, P.P., Bagley, A.F., Markhard, A.L., and Sabatini, D.M. (2006). Prolonged rapamycin treatment inhibits mTORC2 assembly and Akt/PKB. Mol. Cell *22*, 159–168.

Scheijen, B., Ngo, H.T., Kang, H., and Griffin, J.D. (2004). FLT3 receptors with internal tandem duplications promote cell viability and proliferation by signaling through Foxo proteins. Oncogene *23*, 3338–3349.

Seoane, J., Le, H.V., Shen, L., Anderson, S.A., and Massague, J. (2004). Integration of Smad and forkhead pathways in the control of neuroepithelial and glioblastoma cell proliferation. Cell *117*, 211–223.

Subramanian, A., Tamayo, P., Mootha, V.K., Mukherjee, S., Ebert, B.L., Gillette, M.A., Paulovich, A., Pomeroy, S.L., Golub, T.R., Lander, E.S., and Mesirov, J.P. (2005). Gene set enrichment analysis: a knowledge-based approach for interpreting genome-wide expression profiles. Proc. Natl. Acad. Sci. USA *102*, 15545–15550.

Tran, H., Brunet, A., Grenier, J.M., Datta, S.R., Fornace, A.J., Jr., DiStefano, P.S., Chiang, L.W., and Greenberg, M.E. (2002). DNA repair pathway stimulated by the forkhead transcription factor FOXO3a through the Gadd45 protein. Science *296*, 530–534.

Yilmaz, O.H., Valdez, R., Theisen, B.K., Guo, W., Ferguson, D.O., Wu, H., and Morrison, S.J. (2006). Pten dependence distinguishes haematopoietic stem cells from leukaemia-initiating cells. Nature *441*, 475–482.

Zhang, J., Grindley, J.C., Yin, T., Jayasinghe, S., He, X.C., Ross, J.T., Haug, J.S., Rupp, D., Porter-Westpfahl, K.S., Wiedemann, L.M., et al. (2006). PTEN maintains haematopoietic stem cells and acts in lineage choice and leukaemia prevention. Nature *441*, 518–522.

Accession Numbers

The microarray data can be found in the Gene Expression Omnibus (GEO) of NCBI at http://www.ncbi.nlm.nih.gov/geo/ through accession number GSE6623.